

# Processing of epitaxial $\text{LiMn}_2\text{O}_4$ thin film on $\text{MgO}(110)$ through metalorganic precursor

Yumi H. Ikuhara<sup>a)</sup> and Yuji Iwamoto<sup>a)</sup>

*Fine Ceramics Research Association, Synergy Ceramics Laboratory, 2-4-1 Mutsuno, Atsuta-ku, Nagoya, 456-8587, Japan*

Koichi Kikuta and Shin-ichi Hirano

*Graduate School of Engineering, Nagoya University, Furo-cho, Chikusa-ku, Nagoya, 464-8603, Japan*

(Received 21 April 2000; accepted 6 September 2000)

Epitaxial  $\text{LiMn}_2\text{O}_4$  was successfully synthesized by coating a [Li–Mn–O] metalorganic precursor solution onto  $\text{MgO}(110)$  substrates at temperatures as low as  $350^\circ\text{C}$ . Cross-sectional transmission electron microscopy observation revealed that the orientation relationship between  $\text{LiMn}_2\text{O}_4$  and  $\text{MgO}$  was  $(111)_{\text{LiMn}_2\text{O}_4} // (111)_{\text{MgO}}$ ,  $(110)_{\text{LiMn}_2\text{O}_4} // (110)_{\text{MgO}}$ , and  $[112]_{\text{LiMn}_2\text{O}_4} // [112]_{\text{MgO}}$ , which resulted in the  $(111)_{\text{LiMn}_2\text{O}_4}$  planes growing perpendicular to the surface plane of  $\text{MgO}$ . The interface structure consisted of (111) layers of Mn atoms in the  $\text{LiMn}_2\text{O}_4$  crystal aligned with the Mg atoms in the (111) planes of the  $\text{MgO}$  substrate when viewed along the [112] direction.

## I. INTRODUCTION

In recent years, there has been considerable interest in high energy density rechargeable batteries for use in electronic devices. The increase in demand for light-weight portable equipment means that microbatteries must be developed as power sources. Intensive efforts have been directed at fabricating the cell components of these all-solid-state microbatteries, particularly by thin film techniques.

$\text{LiMn}_2\text{O}_4$  spinel,<sup>1–10</sup> the layered compound  $\text{LiCoO}_2$ <sup>11,12</sup> and  $\text{LiNiO}_2$ <sup>13–15</sup> have been extensively investigated for use as cathodic materials in lithium secondary batteries because they all possess the characteristic electrochemical property of intercalation and deintercalation of lithium ions into their crystal structure. In each case, it has been demonstrated that the lithium ions are reversibly inserted between the layered planes. To facilitate the intercalation process in microbatteries, it is beneficial to prepare a lithiated intercalation cathode film with the intercalated plane perpendicular to the surface of the substrate.

Several lithium intercalation compounds have been fabricated in thin film form by techniques such as chemical vapor deposition, evaporation, and sputtering.<sup>16–23</sup> These thin films all have an amorphous or random polycrystalline structure, since a microstructurally controlled

thin film has not yet been prepared. Chemical processing via a solution route using metalorganic precursors is advantageous for preparing thin films with desired stoichiometry, controlled purity, and compositional homogeneity.<sup>24</sup> If an appropriate precursor solution and substrate are chosen in terms of the lattice parameter and crystal structure of the desired compound, microstructurally controlled or highly oriented thin films can be fabricated.

In this study, we report on the preparation of lithium manganese oxide thin film using a metalorganic precursor solution. In this process, we focus on the fabrication of an epitaxial thin film with the (111) intercalated plane perpendicular to the surface of the substrate. The microstructure of the epitaxial  $\text{LiMn}_2\text{O}_4$  thin film was further investigated by interface analysis methods.

## II. EXPERIMENTAL PROCEDURE

### A. $\text{LiMn}_2\text{O}_4$ thin film processing

Starting metalorganic precursors for the fabrication of  $\text{LiMn}_2\text{O}_4$  were  $\text{LiOCH}(\text{CH}_3)_2$  and  $\text{Mn}(\text{OC}_2\text{H}_5)_2$  with 2-ethoxyethanol [ $\text{C}_2\text{H}_5\text{OC}_2\text{H}_4\text{OH}$ ; (EGMEE)] as the solvent. EGMEE was dried over molecular sieves and distilled prior to use. The chemical modification reactions of the metalorganic precursors were carried out under dry nitrogen atmosphere. The metalorganic precursors were dissolved in EGMEE and refluxed at  $135^\circ\text{C}$  for 3 h. The alkoxy ligands in  $\text{LiOCH}(\text{CH}_3)_2$  and  $\text{Mn}(\text{OC}_2\text{H}_5)_2$  were modified to give  $\text{LiOC}_2\text{H}_4\text{OC}_2\text{H}_5$  and  $\text{Mn}(\text{OC}_2\text{H}_4\text{OC}_2\text{H}_5)_4$  by complete reaction.<sup>10,25</sup> After the

<sup>a)</sup>Present address: Japan Fine Ceramics Center, Research and Development Laboratory, 2-4-1 Mutsuno, Atsuta-ku, Nagoya, 456-8587, Japan.

solutions were cooled to room temperature, these two solutions were condensed in a rotary evaporator and added to fresh EGME solution to remove the subreacted products of  $(\text{CH}_3)_2\text{CHOH}$  and  $\text{C}_2\text{H}_5\text{OH}$ .

A homogeneous metalorganic  $[\text{Li-Mn-O}]$  precursor solution was prepared by vigorously mixing the 0.025 M  $\text{LiOC}_2\text{H}_4\text{OC}_2\text{H}_5$  in EGME with 0.05 M  $\text{Mn}(\text{OC}_2\text{H}_4\text{OC}_2\text{H}_5)_4$  in EGME for 1 h at room temperature, followed by repeated distillation using EGME. The  $[\text{Li-Mn-O}]$  precursor solution was then condensed to about 0.1 M and 0.3 M by placing it in a vacuum with a rotary evaporator to remove solvent.

The single-crystal  $\text{MgO}(110)$  substrates were cleaned ultrasonically in ethanol and acetone, soaked in EGME, then dried with nitrogen gas.  $\text{LiMn}_2\text{O}_4$  precursor films were fabricated from brown-colored  $[\text{Li-Mn-O}]$  metalorganic precursor solution by spin coating (Model K-359SD, Kyowariken Co. Ltd. Tokyo, Japan) onto the cleaned single-crystal  $\text{MgO}(110)$  substrates (Tateho Chemical. Co. Ltd. Tokyo, Japan) at a spinning speed of 2000 rpm for 20 s under flowing nitrogen gas.

## B. Crystallization of $\text{LiMn}_2\text{O}_4$ thin films

After coating thin films onto the  $\text{MgO}(110)$  substrates, samples were carefully transferred to a single-zone tube furnace (Model KTF045, Koyo-Lindberg Co. Ltd., Tokyo, Japan) and then heated to 170 °C for 30 min to remove the organic ligands and subsequently heated

further at a rate of 5 °C/min to 350, 500, or 700 °C and annealed for 1 h in oxygen atmosphere. X-ray diffraction (XRD) measurements on heat-treated film were performed with  $\text{Cu K}\alpha$  radiation using a Rint2000 (Rigaku, Tokyo, Japan) diffractometer equipped with monochromator, operating at 30 kV and 50 mA. Pole-figure measurements were performed with a pole-figure attachment using the Schulz method to evaluate the film orientation.

## C. Microstructure observation of $\text{LiMn}_2\text{O}_4$ thin films

The morphology of the precursor derived thin film after being heat treated at 700 °C was characterized by transmission electron microscopy (TEM). For cross-

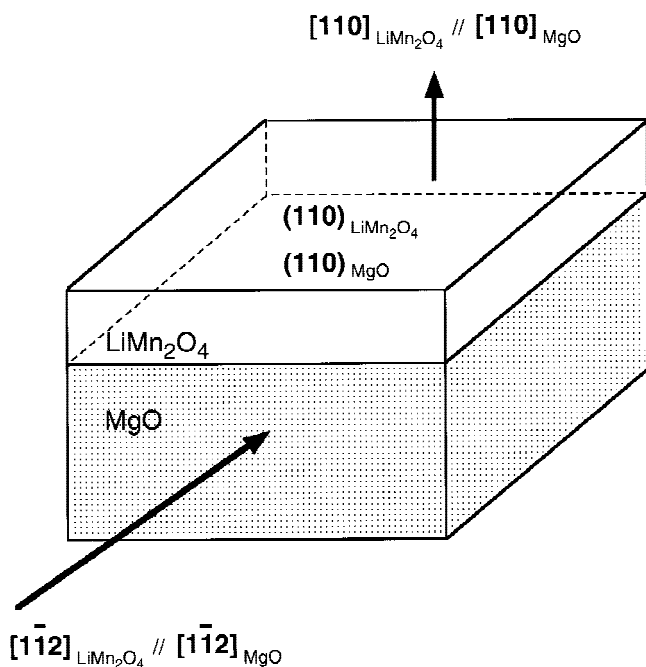


FIG. 1. Geometry of the  $\text{LiMn}_2\text{O}_4$ - $\text{MgO}$  interface. The interface plane is parallel to the (110) plane of  $\text{MgO}$  and  $\text{LiMn}_2\text{O}_4$ . TEM observation was performed from cross-sectional directions:  $[\bar{1}\bar{1}2]_{\text{L}}//[\bar{1}\bar{1}2]_{\text{M}}$ .

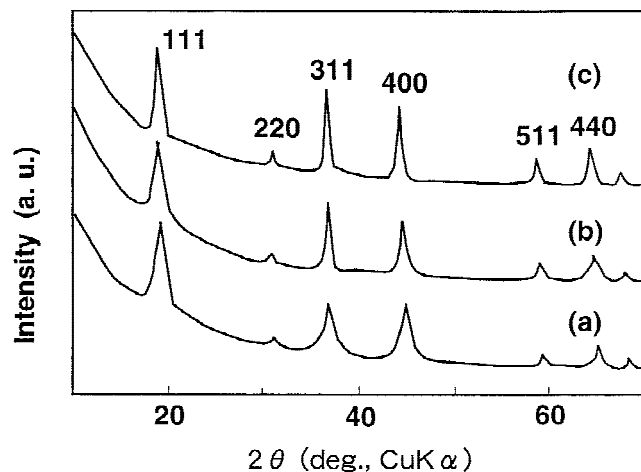


FIG. 2. X-ray diffraction patterns of the films fabricated by coating of the 0.3 M precursor solution followed by heat treatment at (a) 350 °C, (b) 500 °C, and (c) 700 °C.

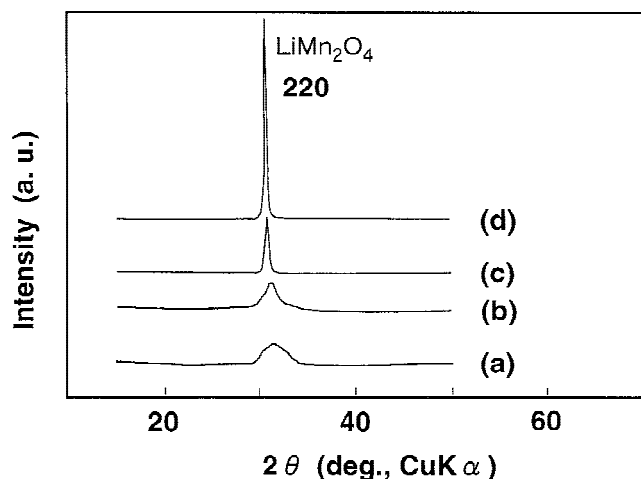


FIG. 3. X-ray diffraction patterns of the films fabricated by coating of the 0.1 M precursor solution followed by heat treatment at (a) 350 °C, (b) 500 °C, and (c) 700 °C, after one cycle, and (d) 700 °C with additional coating and heating cycles.

sectional observation by TEM, samples were prepared as follows. Each sample was first oriented by x-ray Laue back reflection from the substrate side and cut using a diamond saw parallel to the (112) plane. Then two of the cut pieces were glued together using Petropoxi 154 (Marto Inc., Tokyo, Japan) with the film surfaces facing each other. These 'sandwiches' were cut into bars of length approximately 1.5 mm, polished to about 0.1 mm thick, and then attached with epoxy to Mo rings for reinforcement. These were subsequently dimpled to a thickness of about 20  $\mu\text{m}$  and finally thinned by ion beam sputtering at 4–5 kV, using a cold stage (cooled with liquid  $\text{N}_2$ ) to minimize damage to the specimens. Shields were used to protect the interfaces and to reduce the effect of the different milling rates of  $\text{LiMn}_2\text{O}_4$  and  $\text{MgO}$ . In all the micrographs presented in this paper, the growth direction is upward. Conventional and high-resolution electron microscopic observations were performed using a JEOL 2010 electron microscope (JEOL Co, Ltd., Tokyo, Japan) operating at 200 kV with a point to point resolution of about

0.194 nm. The  $\text{LiMn}_2\text{O}_4$  and  $\text{MgO}$  interfaces were characterized from the  $[1\bar{1}2]_{\text{LiMn}_2\text{O}_4} // [1\bar{1}2]_{\text{MgO}}$  direction (Fig. 1).

### III. RESULTS AND DISCUSSION

#### A. Synthesis of $\text{LiMn}_2\text{O}_4$ thin films

Firstly, thin film formation was investigated by changing the concentration of the [Li–Mn–O] metalorganic precursor solutions. Figures 2(a), 2(b), and 2(c) show the XRD patterns of the thin films after heat treatment at 350, 500, and 700  $^\circ\text{C}$ , respectively, in oxygen atmosphere using the 0.3 M precursor solution. Single phase lithium manganese spinel thin film could be prepared by heat treatment at a temperature as low as 350  $^\circ\text{C}$ , where peaks corresponding to (111), (220), (311), (400), (511), and (440) reflections were detected. These results coincide with those obtained by powder processing.<sup>10</sup> XRD analysis revealed that polycrystalline  $\text{LiMn}_2\text{O}_4$  thin films were prepared at all temperatures up to 700  $^\circ\text{C}$ . The

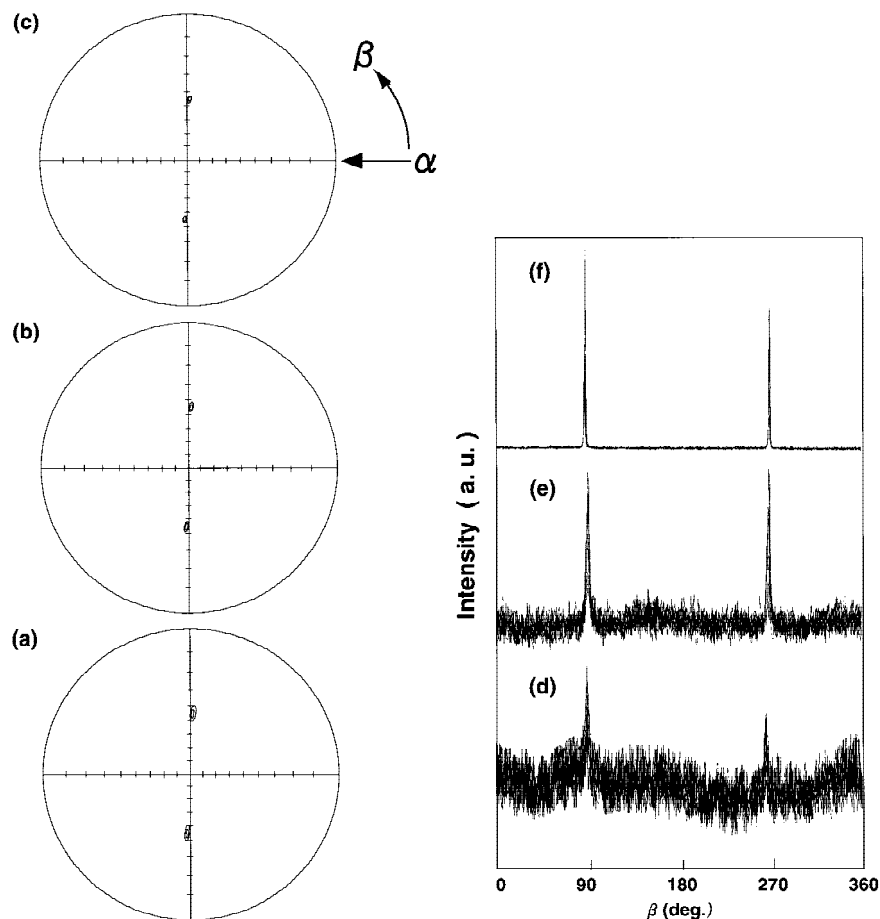


FIG. 4. Pole figures of  $\text{LiMn}_2\text{O}_4$  films prepared on  $\text{MgO}(110)$  substrates by coating of the 0.1 M precursor solution followed by heat treatment at (a) 350  $^\circ\text{C}$ , (b) 500  $^\circ\text{C}$ , and (c) 700  $^\circ\text{C}$ , and the corresponding overwritten x-ray diffraction patterns of films heat treated at (d) 350  $^\circ\text{C}$ , (e) 500  $^\circ\text{C}$ , and (f) 700  $^\circ\text{C}$ .

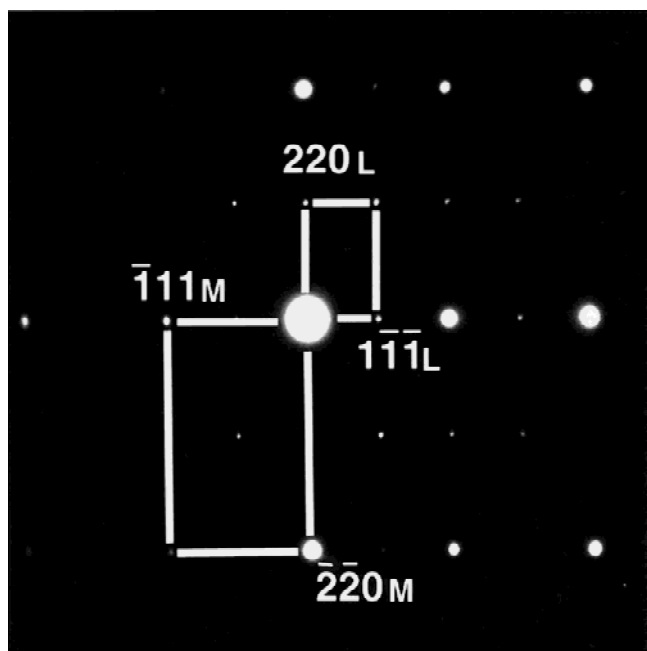


FIG. 5. Selected-area diffraction pattern of the  $\text{LiMn}_2\text{O}_4$ - $\text{MgO}$  system projected along  $[1\bar{1}\bar{2}]_L//[1\bar{1}\bar{2}]_M$  cross-sectional directions.  $\text{LiMn}_2\text{O}_4$  thin film was fabricated by coating the 0.1 M precursor solution followed by heat treatment at 700 °C.

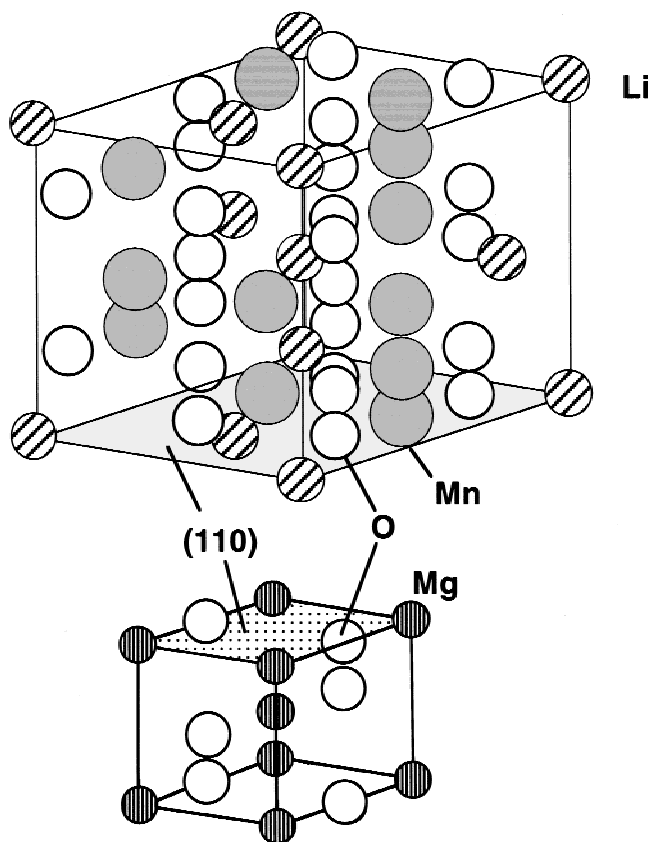


FIG. 6. Schematic representation of the orientation relationship between  $\text{LiMn}_2\text{O}_4$  and  $\text{MgO}$  substrate. The (110) face of  $\text{LiMn}_2\text{O}_4$  is parallel to the (110) face of  $\text{MgO}$ .

strong peak at  $2\theta = 18.76^\circ$  corresponds to the (111) plane with an interplanar distance of  $d = 0.476$  nm. It therefore appears that using a higher concentration solution results in a large number of nuclei forming in the upper part of the film where they are not constrained to grow epitaxially during heat treatment.

When a lower concentration precursor solution such as 0.1 M was used for the spin coating, only the (110) peak could be detected in samples prepared at 350, 500, and 700 °C [Figs. 3(a), 3(b), and 3(c)] by XRD. This indicates that the (110) plane of  $\text{LiMn}_2\text{O}_4$  is highly oriented on the  $\text{MgO}(110)$  substrate, since in polycrystalline  $\text{LiMn}_2\text{O}_4$  powder (JCPDS Card No. 35-782), the ratio of the intensity of the (110) peak to that of the maximum

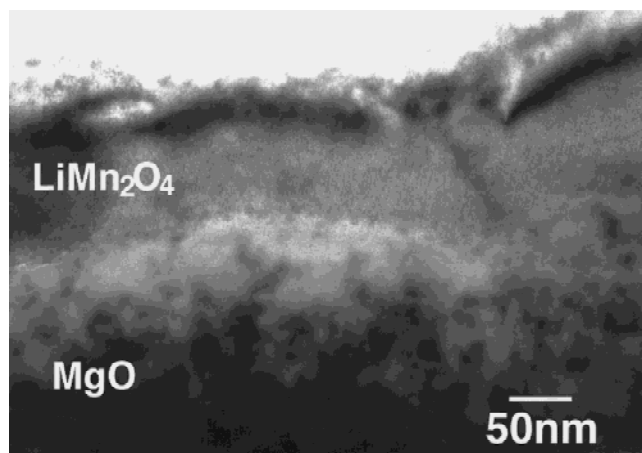


FIG. 7. Bright-field transmission electron micrograph of the  $\text{LiMn}_2\text{O}_4$  film on the  $\text{MgO}(110)$  substrate heat treated at 700 °C, obtained with the electron beam aligned along the  $[1\bar{1}\bar{2}]_L//[1\bar{1}\bar{2}]_M$  direction. The growth occurred in an upward direction.

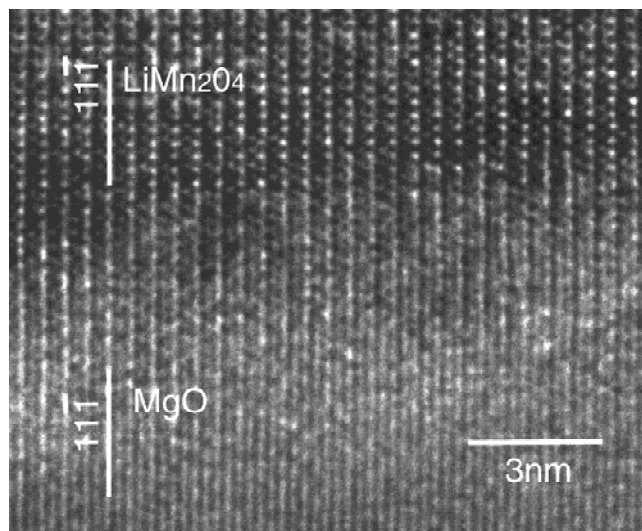


FIG. 8. Cross-sectional high-resolution electron micrograph of the  $\text{LiMn}_2\text{O}_4$ - $\text{MgO}$  interface heat treated at 700 °C, with the incident electron beam parallel to  $[1\bar{1}\bar{2}]_L//[1\bar{1}\bar{2}]_M$ .

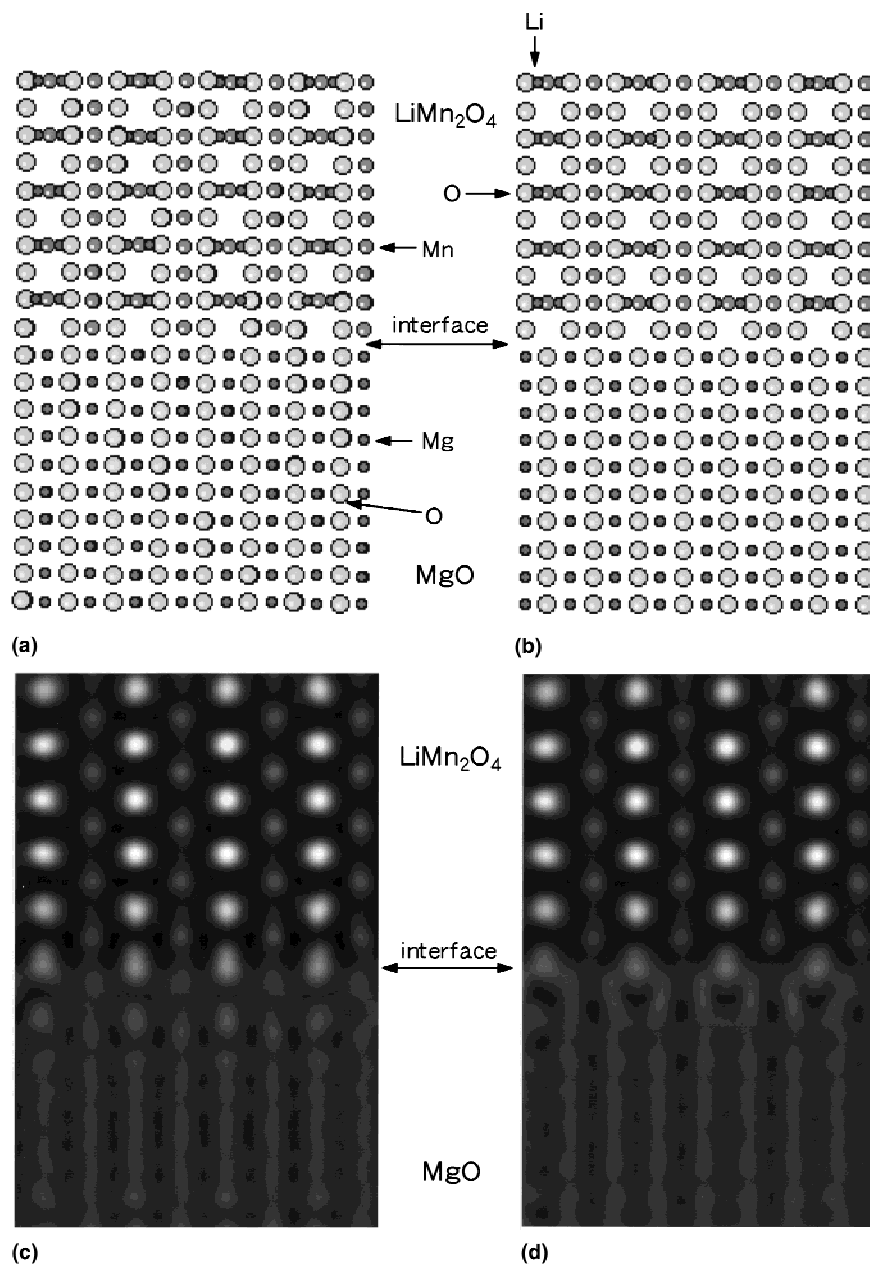


FIG. 9. (a) Projected  $\text{LiMn}_2\text{O}_4/\text{MgO}$  interfacial structure models of (a) and (b) along the  $[1\bar{1}2]_{\text{L}}/[1\bar{1}2]_{\text{M}}$  direction; (c) and (d) are computer-simulated images based on the structural models of (a) and (b), respectively.

peak (111) is 1:100. Furthermore, with additional 0.1 M solution coating and heating at  $700^\circ\text{C}$ , the intensity of the (110) peak increased as shown in Fig. 3(d), because the volume of oriented  $\text{LiMn}_2\text{O}_4$  increased.

These results show that it is possible to successfully coat multiple layers of the oriented thin film by careful selection of the substrate and precursor concentration.

### B. Crystal orientation of $\text{LiMn}_2\text{O}_4$ thin film

To confirm the epitaxy of the thin film, pole-figure measurements were performed, as this is a powerful method for obtaining the three-dimensional information

about crystal structure. The crystallographic oriented structure of the  $\text{LiMn}_2\text{O}_4$  thin film prepared from 0.1 M precursor solution on  $\text{MgO}(110)$  was characterized using the (400) reflection.

Figure 4 shows pole figures of the  $\text{LiMn}_2\text{O}_4$  on  $\text{MgO}(110)$  substrates heat treated at (a)  $350^\circ\text{C}$ , (b)  $500^\circ\text{C}$ , and (c)  $700^\circ\text{C}$  when the (400) plane of  $\text{LiMn}_2\text{O}_4$  was set normal to the x-ray direction, where the  $\text{LiMn}_2\text{O}_4$  the  $\text{MgO}(110)$  substrate is inclined at  $43^\circ$  to the horizontal. Figures 4(d), 4(e), and 4(f) show the corresponding overwritten XRD patterns in the range of  $\alpha$ -scan from  $0^\circ$  to  $90^\circ$  with the range of  $\beta$ -scan from  $0^\circ$  to  $360^\circ$ . The term

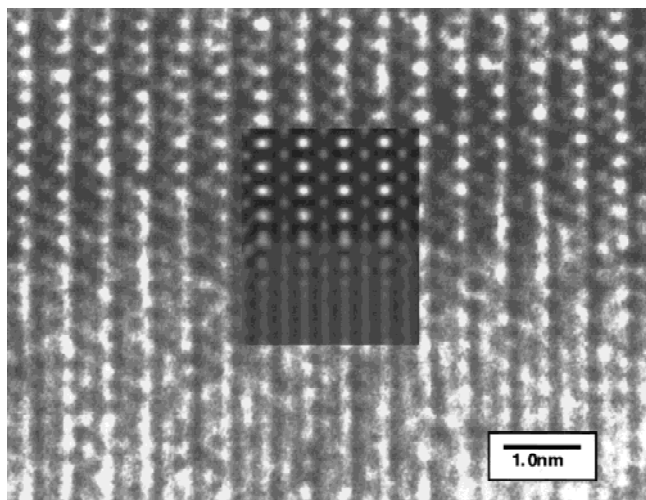


FIG. 10. Experimental HREM images of the LiMn<sub>2</sub>O<sub>4</sub>-MgO interface heat treated at 700 °C, projected along the  $[1\bar{1}2]_L//[1\bar{1}2]_M$  direction. The inset is the computer-simulated image shown in Fig. 9(c).

$\beta$  is the rotation axis perpendicular to the film plane, and  $\alpha$  is the rotation axis perpendicular to  $\beta$  and  $\theta$ . There are six reflections; (400),  $(\bar{4}00)$ , (040),  $(0\bar{4}0)$ , (004),  $(00\bar{4})$ , for {400} and their angles to the (220) plane are 45°, 135°, 45°, 135°, 90°, and 90°, respectively. Since only (400) and (040) have angles smaller than 90°, these reflections with two fold symmetry between LiMn<sub>2</sub>O<sub>4</sub> and MgO (110) appear as two spots along  $\beta$  at  $\alpha = 45^\circ$  as shown in Figs. 4(a), 4(b), and 4(c), indicating that oriented LiMn<sub>2</sub>O<sub>4</sub> thin film on MgO(110) was prepared by heat treatment at 350, 500, and 700 °C. The combination of XRD (Fig. 3) and pole figure analysis (Fig. 4) results show clearly that epitaxial growth takes place even at 350 °C. Nevertheless, the degree of orientation is not as high for the film formed at 350 °C, compared with those formed at higher temperatures.

These results indicate that nucleation and crystallization commence at a low temperature on the MgO(110) substrate by this method using metalorganic precursor solution and that the crystallization proceeds at higher temperatures while maintaining the homogeneity of the crystal structure.

### C. Orientation relationship between LiMn<sub>2</sub>O<sub>4</sub> thin film and MgO

Both LiMn<sub>2</sub>O<sub>4</sub> and MgO have cubic crystal structures; LiMn<sub>2</sub>O<sub>4</sub> is a spinel (space group,  $Fd\bar{3}m$ ) while MgO has a sodium chloride structure (space group,  $Fm\bar{3}m$ ). In this section, the orientation relationship between LiMn<sub>2</sub>O<sub>4</sub> film and MgO substrate being heat treated at 700 °C was investigated by transmission electron microscopy (TEM). In the following discussion, LiMn<sub>2</sub>O<sub>4</sub> and MgO are denoted by the

subscripts L and M, respectively, to simplify identification of crystal planes and directions in each material.

Figure 5 shows the selected-area diffraction patterns of the cross-sectional LiMn<sub>2</sub>O<sub>4</sub> thin film on MgO substrate heat treated at 700 °C with the incident electron beam parallel to  $[1\bar{1}2]_L//[1\bar{1}2]_M$  directions. According to this diffraction pattern, the orientation relationship between LiMn<sub>2</sub>O<sub>4</sub> and MgO is

$$\begin{aligned} (1\bar{1}\bar{1})_L & // (1\bar{1}\bar{1})_M \\ (110)_L & // (110)_M \\ [1\bar{1}2]_L & // [1\bar{1}2]_M \end{aligned}$$

Since the lattice parameters of LiMn<sub>2</sub>O<sub>4</sub> and MgO are 0.8247 and 0.4213 nm, respectively, the area of the (110) face of the MgO unit cell is very nearly one-quarter that of the LiMn<sub>2</sub>O<sub>4</sub> unit cell. Thus,  $(110)_L$  can fit very well onto the surface of  $(110)_M$ . Here, the misfit parameter  $f = 2 [d(222)_L - d(111)_M]/[d(111)_M]$  between the parallel  $(222)_L$  and  $(111)_M$  planes, which are perpendicular to the interface, is 2%. The question as to whether Mn atoms align on the Mg atoms or not will be addressed later.

The orientation relationship is indicated in Fig. 6, which shows schematically the interface between  $(110)_L$  and  $(110)_M$ . Cross-sectional directions such as  $[1\bar{1}2]_L//[1\bar{1}2]_M$ , which lie in the  $(110)_M$  plane, are exactly parallel to the interface and are suitable directions for high-resolution electron microscopy (HREM) observations.

Figure 7 shows a bright-field image of the LiMn<sub>2</sub>O<sub>4</sub> film heat treated at 700 °C on the MgO(110) substrate obtained with the electron beam aligned along the  $[1\bar{1}2]_L//[1\bar{1}2]_M$  zone axis. It can be seen that the LiMn<sub>2</sub>O<sub>4</sub>-MgO interface has a wavy structure and is not atomically smooth in some regions, while the thickness of the heat-treated film is about 100 nm.

Figure 8 is a cross-sectional HREM image of the interface region. According to the selected area diffraction pattern in Fig. 5 and the HREM image in Fig. 8,  $(111)_L$  is grown epitaxially perpendicular to the  $(110)_M$  surface, which corresponds to the results of the pole figure. The thermal decomposition of the precursor and nucleation of the LiMn<sub>2</sub>O<sub>4</sub> occurred at low temperature (approximately 200 °C),<sup>25</sup> and the epitaxial growth was accelerated on the surface of the MgO(110) substrate at temperatures up to 700 °C. In the next section, we discuss the atomic structure model at the LiMn<sub>2</sub>O<sub>4</sub>/MgO interface based on the orientation relationship results and the HREM image.

### D. Atomic structure of the LiMn<sub>2</sub>O<sub>4</sub>-MgO interface

Since the misfit between LiMn<sub>2</sub>O<sub>4</sub> and MgO is about 2%, the model was constructed to expand the LiMn<sub>2</sub>O<sub>4</sub> so as to exactly fit the MgO atomic alignment of the

substrate to form a coherent interface. Two possibilities were considered for the position of Mn atoms on the (110) surface of MgO. Figures 9(a) and 9(b) show two projected interfacial structure models along the  $[1\bar{1}2]_{\text{L}}//[1\bar{1}2]_{\text{M}}$  beam directions using supercells where Mn atoms on the (110) surface of MgO are located directly above the Mg atoms (model I), or on the O atoms (model II), in the projected image. In constructing the supercells in Fig. 9, the separation between the two crystals was assumed to be such that the shortest interatomic distance corresponds to the bond length in an MgO crystal. On this basis, the shortest interatomic distance in model I (or II) of Fig. 9 is 0.210 nm. Computer simulations were performed using the supercells. The supercell lattice parameters were  $1.823 \times 2.828 \times 2.000 \text{ nm}^3$  for model I and model II.

Figures 9(c) and 9(d) are computer-simulated images of the interface models shown in Figs. 9(a) and 9(b) respectively, for a crystal thickness of 9 nm and a defocus of  $-7 \text{ nm}$ . These calculations were actually performed over a range of thickness from 5 to 15 nm, and a range of defocus from  $-5$  to  $-30 \text{ nm}$ . The best fits to the experimental images in the direction  $[1\bar{1}2]_{\text{L}}//[1\bar{1}2]_{\text{M}}$  were obtained for model I. This indicates that there is a good match between model I and the experimental image. A comparison of the simulated HREM images of model I with the experimental images in the  $[1\bar{1}2]$  directions is shown in Fig. 10. As can be seen, there are reasonable matches between the simulated and experimental images, indicating that model I is closer to the actual structure of the  $\text{LiMn}_2\text{O}_4$ -MgO interface. Hence, in the present system, the Mn atoms in the (111) layers are most likely aligned with the Mg atoms in the (111) planes of the MgO substrate when viewed in the  $[1\bar{1}2]$  direction. This can be understood in terms of the close match between the spinel and sodium chloride crystal structures, which encourages the  $\text{LiMn}_2\text{O}_4$  crystallites to grow essentially as an extension of the cubic MgO crystal.

#### IV. CONCLUSIONS

Randomly oriented polycrystalline and epitaxial thin films of  $\text{LiMn}_2\text{O}_4$  on  $\text{MgO}(110)$  substrates were prepared by controlling the concentration of the synthesized  $[\text{Li-Mn-O}]$  metalorganic precursor solution followed by heat treatment at temperatures as low as  $350 \text{ }^\circ\text{C}$ . When 0.3 M precursor solution was used for coating, the thin films heat treated at 350, 500, and  $700 \text{ }^\circ\text{C}$  consisted of randomly oriented polycrystalline  $\text{LiMn}_2\text{O}_4$ . However, when 0.1 M precursor solution was used, epitaxial  $\text{LiMn}_2\text{O}_4$  thin films could be obtained by heat treatment at 350, 500, and  $700 \text{ }^\circ\text{C}$ .

The interface structure of epitaxial  $\text{LiMn}_2\text{O}_4$  on  $\text{MgO}(110)$  heat treated at  $700 \text{ }^\circ\text{C}$  has been investigated by conventional and high-resolution TEM. Cross-

sectional TEM reveals that the orientation relationship between MgO and  $\text{LiMn}_2\text{O}_4$  is  $(111)_{\text{L}}// (111)_{\text{M}}$ ,  $(110)_{\text{L}}// (110)_{\text{M}}$   $[112]_{\text{L}}// [112]_{\text{M}}$ , which results in the  $(111)_{\text{L}}$  planes growing perpendicular to the surface plane of MgO. Since the area of one face of the cubic MgO unit cell is very nearly quarter that of the  $\text{LiMn}_2\text{O}_4$  unit cell face, this orientation relationship results in a good fit between the Mn atomic layer of the film and the Mg atomic layer of the substrate at the interface. Hence, when the epitaxial  $\text{LiMn}_2\text{O}_4$  film is prepared on  $\text{MgO}(110)$ , the (111) layers of Mn atoms align themselves above the (111) layers of Mg atoms in the substrate.

#### ACKNOWLEDGMENTS

This work was entrusted by NEDO as part of the Synergy Ceramics Project under the Industrial Science and Technology Frontier (ISTF) Program promoted by AIST, MITI, Japan. The authors are members of the Joint Research Consortium of Synergy Ceramics.

#### REFERENCES

1. M.M. Thackeray, P.J. Johnson, L.A. de Picciotto, P.G. Bruce, and J.B. Goodenough, *Mater. Res. Bull.* **19**, 179 (1984).
2. S. Bach, J.P. Pereira-Ramos, N. Baffier, and R. Messina, *Electrochim. Acta* **37**, 1301(1992).
3. M.H. Rossouw, A. de Kock, L.A. de Picciotto, M.M. Thackeray, W.I.F. David, and R.M. Ibberson, *Mater. Res. Bull.* **25**, 173 (1990).
4. T. Ohzuku, M. Kitagawa, and H. Taketsugu, *J. Electrochem. Soc.* **137**, 769 (1990).
5. H. Huang and P.G. Bruce, *J. Electrochem. Soc.* **141**, 185 (1994).
6. J.M. Tarascon, W.R. McKinnon, F. Coowar, T.N. Bowmer, G. Amatucci, and D. Guyomard, *J. Electrochem. Soc.* **141**, 1421 (1994).
7. R.J. Gummow, A. de Kock, and M.M. Thackeray, *Solid State Ionics* **69**, 59 (1994).
8. C. Masquelier, M. Tabuchi, K. Ando, R. Kanno, Y. Kobayashi, Y. Maki, O. Nakamura, and J.B. Goodenough, *J. Solid State Chem.* **23**, 256 (1996).
9. D. Guyomard and J.M. Tarascon, *J. Electrochem. Soc.* **139**, 937 (1992).
10. Y.H. Ikuhara, Y. Iwamoto, K. Kikuta, and S. Hirano, *J. Mater. Res.* **14**, 3102 (1999).
11. J.N. Reimers and J.R. Dahn, *J. Electrochem. Soc.* **139**, 2091 (1992).
12. R.J. Gummow, D.C. Liles, M.M. Thackeray, and W.I.F. David, *Mater. Res. Bull.* **28**, 1177 (1993).
13. M.G.S.R. Thomas, W.I.F. David, J.B. Goodenough, and P. Gloves, *Mater. Res. Bull.* **20**, 1137 (1985).
14. J.R. Dahn, U. von Sacken, and C.A. Michael, *Solid State Ionics* **44**, 87 (1990).
15. A. Hirano, R. Kanno, Y. Kawamoto, Y. Takeda, K. Yamaura, M. Takano, K. Ohyama, M. Ohashi, Y. Yamaguchi, *Solid State Ionics* **78**, 123 (1995).
16. P. Fragnaud, R. Nagarajan, D.M. Scaleich, and D. Vujic, *J. Power Sources* **54**, 362 (1995).
17. F.K. Shokoohi, J.M. Tarascon, and B.J. Wilkens, *Appl. Phys. Lett.* **59**, 1260 (1991).

18. F.K. Shokoohi, J.M. Tarascon, B.J. Wilkens, D. Guyomard, and C.C. Chang, *J. Electrochem. Soc.* **139**, 1845 (1992).
19. M. Antaya, J.R. Dahn, J.S. Preston, E. Rosen, and J.N. Reimers, *J. Electrochem. Soc.* **140**, 575 (1993).
20. M. Antaya, K. Cleams, J.S. Preston, J.N. Reimers, and J.R. Dahn, *J. Appl. Phys.* **76**, 2799 (1994).
21. K-H. Hwang, S-H. Lee, and S-K. Joo, *J. Electrochem. Soc.* **41**, 3296 (1994).
22. J.B. Bates, G.R. Gruzalski, N.J. Dadney, C.F. Luck, and X. Yu, *Solid State Ionics* **70/71**, 619 (1994).
23. J.B. Bates, D. Lubben, L.J. Dudney, and F.X. Harf, *J. Electrochem. Soc.* **142**, L149 (1995).
24. Y.H. Ikuhara, Y. Iwamoto, K. Kikuta, S. Hirano, *IONICS* **6**, 156 (2000).
25. Y.H. Ikuhara, Y. Iwamoto, K. Kikuta, and S. Hirano, *Ceram. Trans.* **83**, 53 (1998).